Macromolecules
Cite This: Macromolecules 2018, 51, 9294−9305
Article
pubs.acs.org/Macromolecules

Opposing Effects of Side-Chain Flexibility and Hydrogen Bonding on the Thermal, Mechanical, and Rheological Properties of Supramolecularly Cross-Linked Polyesters

Qianhui Liu,[†] Chao Wang,[‡] Yuanhao Guo,[‡] Chao Peng,[†] Amal Narayanan,[†] Sukhmanjot Kaur,[†] Ying Xu,[†] R. A. Weiss,*[,‡] and Abraham Joy*[,†]

[†]Department of Polymer Science and [‡]Department of Polymer Engineering, The University of Akron, Akron, Ohio 44325, United States

Supporting Information

ABSTRACT: We report the design of a series of polyesters containing pendant secondary amide groups to probe the cumulative effects of hydrogen bonding and chain flexibility on their thermal, mechanical, and rheological properties. Reported studies on polymers with secondary amide groups have usually focused on the effect of hydrogen bonding interactions on the mechanical, self-assembly, or self-healing properties, whereas the effect of chain flexibility has often been overlooked. In an effort to probe the cumulative effects of hydrogen bonding and chain flexibility, in this work polyesters were designed with either one or two pendant secondary amide-propyl groups and compared to a control polyester with one pendant ester-propyl group. The results show that hydrogen bonding increases glass transition temperature (T_g), Young's modulus, and polymer brittleness. But at higher temperature (T_g + 50 °C), rheometry shows that the polyester containing two amide groups has the shortest chain relaxation time and the lowest zero-shear rate viscosity (η_0). These results are counterintuitive, since the polymer with two hydrogen bonding amide groups was expected to relax more slowly and have higher viscosity. Our results demonstrate the opposing effects of side-chain flexibility and hydrogen bonding interactions can be used as a strategy to design materials with desired rheological properties.

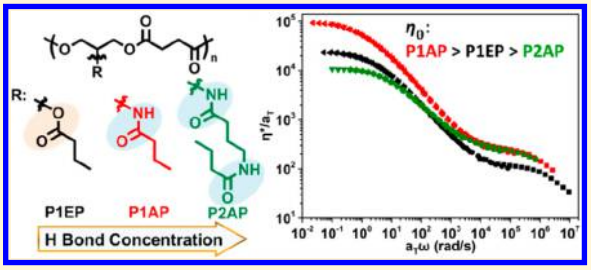

INTRODUCTION

Polymers reinforced through supramolecular forces such as hydrogen bonds are explored widely and used in many fields because of their enhanced mechanical and thermal properties. The dynamic nature of hydrogen bonds endows materials with various interesting behaviors, like viscosity modulation,[1] self-assembly,[2−4] self-healing,[5−8] adhesion,[6,7,9] and reversible properties.[10] The extent of hydrogen bonds could be tuned internally by selecting the type and density of functional groups where hydrogen bonds can form and also by altering external conditions like temperature, humidity, or solvent.[11,12]

In polymers such as polyamides, the secondary amide group is frequently utilized to induce hydrogen bond formation, which in turn plays key roles in determining material properties and functions. For instance, in biological systems, hydrogen bonds play crucial roles in organization of the secondary and tertiary structures of proteins and nucleic acids.[13]

Hydrogen bonds can serve as dynamic cross-links that strengthen the material and limit chain mobility.[14,15] However, secondary amide groups result in flexible chains that can switch easily between conformations due to the large bond angles.[16,17] But the inherent flexibility in secondary amide groups is not often observed as it is overshadowed by hydrogen bonding interaction and other factors. For example, many reports have studied flexibility of proteins and peptides,[18−22] where numerous secondary amides exist in the backbone, but the varied interactions (hydrophobic interactions, salt bridges, and hydrogen bonding)[20] and hierarchical structures of proteins add further complexity to the system.[23] Even for a single polypeptide chain, the flexibility is limited. This is because the C−N bond of the secondary amide group has significant double bond character, and the atoms connecting to C−N bond are coplanar.[24] The internal rotation is limited due to the sequential coplanar arrangements of adjacent amide groups.[25] Additionally, hydrogen bonds in secondary amide-containing polymers such as nylon-6 promote polymer chain alignment into well-ordered structures, which in turn conceals chain flexibility.

Rheological analyses of polymer melts with hydrogen bonded side-chains have been reported. Small-amplitude oscillatory shear (SAOS) measurements provide information regarding the viscoelastic behavior of polymers. The storage modulus (G') corresponds to the stored energy, and the loss modulus (G'') measures the dissipated energy. During SAOS

Received: August 17, 2018
Revised: October 20, 2018
Published: November 13, 2018

DOI: 10.1021/acs.macromol.8b01781
Macromolecules 2018, 51, 9294−9305

analysis, materials are in their linear viscoelastic regions, where the polymer structures are not disturbed. During SAOS analysis of a high molecular mass polymer having entanglements, with increasing frequency the material goes through four regions: terminal region, rubbery region, transition region, and glassy region. The material is more solid-like at higher frequency and more liquid-like at lower frequency. In the terminal region, the polymer chains can move freely, and for a thermally simple polymer, G' is proportional to the square of angular frequency (ω) and G'' is proportional to ω.[26] In the rubbery region, the polymer chains are not deforming but interlock with each other through entanglements. Shabbir et al.[27] synthesized a series of copolymers of *n*-butyl acrylate (nBA) and acrylic acid (AA) with different fractions of P(AA) obtained by hydrolysis of pure P(nBA). Their results showed that hydrogen bonds did not influence the linear viscoelastic behavior of the polymer, except in the terminal region, where $G' \approx G'' \propto \omega^{0.5}$. Lewis and co-workers[28] studied viscoelastic behaviors of copolymers made by *n*-butyl acrylate and various comonomers (acrylic acid, carboxyl ethyl acrylate, aminopyridine, and ureidopyrimidine (Upy)-modified acrylate). They showed that with the increase of hydrogen bonding side group concentration both G' and G'' of the four polymers increased, and copolymers containing weak hydrogen bonding groups behaved as unentangled melts. Nevertheless, a plateau region appeared at intermediate frequencies in the polymer with Upy groups, indicating formation of transient networks, and in the terminal region, $G' \approx G'' \propto \omega^{0.5}$. Osterwinter et al.[29] synthesized polyglycerol where hydrogen bonds can form between hydroxyl groups and its permethylated analogue. Their results showed that polyglycerol had a higher plateau modulus and lower entanglement molecular weight, indicating there were more entanglements with polyglycerol. However, the above studies have not enabled examination of the cumulative effects of both hydrogen bonding interaction and chain flexibility. For example, in the study reported by Shabbir et al., hydrolysis of the nBA groups to the corresponding acrylic acid resulted in a decrease of side-chain flexibility, and with increasing hydrolysis the influence of hydrogen bonds increased while chain flexibility decreased.

To create a polymer system where the influence of both side-chain flexibility and hydrogen bonding can be observed, we prepared amorphous polyesters containing either one ester-propyl group (P(1EP)), one secondary amide-propyl group (P(1AP)), or two secondary amide-propyl groups (P(2AP)) in the side-chain. The polyesters were synthesized by room temperature step-growth polyesterification of succinic acid and glycerol or serinol modified diols catalyzed by carbodiimide coupling.[30] In P(2AP), the three methylene units between the two secondary amide groups increase the distance between amide groups and prevent the formation of sequential coplanar arrangements of amide groups, which increases chain flexibility. At high temperature where the hydrogen bond interactions are weakened, the inherently flexible side-chains serve as "internal diluents", decreasing friction of polymer chains, and improving the rotation of the polymer backbones.[31] This effect is especially obvious with P(2AP) due to its larger side-chain length. With P(1AP) and P(2AP), hydrogen bonds served as dynamic cross-links, increasing material stiffness and brittleness, while at high temperature, the longer flexible side-chain of P(2AP) decreased the modulus and induced faster relaxation as observed from melt rheological analysis. Our studies bear similarities between published reports of polymers with hydrogen bonding side-chains[28,27,32] but also show very distinct behavior from such polymers, especially as it relates to the interplay of chain flexibility and hydrogen bonding.

EXPERIMENTAL SECTION

Materials. 1,3-Dihydroxyacetone was purchased from Ark Pharm Inc. *tert*-Butyldimethylsilyl chloride (TBDMSCl) and 2-aminopropane-1,3-diol (serinol) were purchased from Oakwood Chemicals. Imidazole, butyric anhydride, tetra-*n*-butylammonium fluoride (tBAF, 1 M solution in THF), methyl butyrate, and dioxane were purchased from Alfa Aesar. Sodium borohydride was purchased from BDH Chemicals. 4-(Dimethylamino)pyridine (DMAP) and *N*,*N*′-diisopropylcarbodiimide (DIC) were purchased from Chem-Impex International. 4-Aminobutyric acid was purchased from Acros Organics. Thionyl chloride was purchased from TCI. Triethylamine (TEA) was purchased from EMD Millipore Corp. Succinic acid, methanol, dichloromethane (DCM), and tetrahydrofuran (THF) were purchased from Fisher Chemical. THF and DCM were distilled to remove water before use, and all other reagents were used as received without further purification. 4-(Dimethylamino)pyridinium-4-toluenesulfonate (DPTS) was synthesized based on a previous report[33]. $CDCl_3$ and DMSO-d_6 were purchased from Cambridge Isotope Laboratories, Inc.

Instrumentation. ^{1}H and ^{13}C NMR spectra were recorded with a Varian NMR spectrophotometer (300 MHz). All chemical shifts were reported in ppm relative to solvent residual signal (^{1}H NMR $CDCl_3$ 7.27 ppm; ^{1}H NMR DMSO-d_6 2.5 ppm; ^{13}C NMR $CDCl_3$ 77.16 ppm; ^{13}C NMR DMSO-d_6 39.52 ppm). Weight-average molecular mass (M_w) and molecular mass distribution (dispersity, $Đ$) were measured by a HLC-8320 GPC from TOSOH equipped with RI detector using polystyrene as standard and DMF as eluent at a flow rate of 1 mL/min. The glass transition temperature (T_g) of the polymers was measured by differential scanning calorimetry (DSC) using a TA Q2000 instrument at a scanning rate of 10 °C/min. FT-IR spectroscopies were recorded with FT-IR (Thermo Nicolet 380). The water contact angle measurement was done with a contact angle goniometer (Ramé-Hart). Polymer thin films were prepared by solvent casting using a spin coater (20.0 mg of polymer in 1 mL of solvent; $CHCl_3$ for P(1EP), MeOH for P(1AP) and P(2AP)). Rheological properties of polymers were performed with an ARES-G2 rotational rheometer with fixed strain. Mechanical properties of the polymers were measured by an Instron 5567. Morphology of samples after tensile testing was observed by a scanning electron microscope (SEM JSM7401) and an optical microscope (Leitz Laborlux 12 polarized light microscope).

Synthesis of 2-Butyryloxypropane-1,3-diol. 1,3-Dihydroxyacetone (2.0 g, 0.022 mol), TBDMSCl (8.03 g, 0.053 mol), and imidazole (7.56 g, 0.11 mol) were added into a 200 mL round-bottom flask equipped with a magnetic stir bar. Anhydrous THF (50 mL) was added into the flask via a syringe under a N_2 atmosphere. The mixture was stirred for 12 h at room temperature with N_2 protection. The reaction mixture was concentrated under vacuum. The compound was extracted by ethyl acetate (150 mL), followed by washing with water (50 mL, 2×), 10% HCl solution (50 mL, 2×), and brine (50 mL, 1×) and dried over anhydrous Na_2SO_4. The filtrate was concentrated under vacuum and purified by silica column chromatography (10% ethyl acetate and 90% hexane, R_f = 0.5) followed by silica column chromatography (40% DCM, 60% hexane, R_f = 0.6) to give a colorless liquid **1A** (5.2 g, 74%).

^{1}H NMR (300 MHz, $CDCl_3$), δ (ppm): 0.08 (s, 12H), 0.91 (s, 18H), 3.65 (t, J = 3 Hz, 4H).

TBDMS protected 1,3-dihydroxyacetone **1A**(5.0 g, 0.0157 mol) was dissolved in a mixture of regular THF (48 mL) and water (3.2 mL), and the flask was cooled with an ice bath. $NaBH_4$ (1 equiv, 0.6 g, 0.0157 mol) was added into the flask. The mixture was stirred for 30 min at 0 °C. Thin-layer chromatography (TLC) was used to monitor the reaction process (10% EtOAc in hexane and stained with $KMnO_4$). After the reaction was completed, acetic acid was added dropwise to consume the excess of $NaBH_4$. THF was removed under

DOI: 10.1021/acs.macromol.8b01781
Macromolecules 2018, 51, 9294−9305

vacuum, and the product was extracted by $CHCl_3$. The organic layer was washed by water (50 mL, 2×), saturated $NaHCO_3$ (50 mL, 2×), and brine (50 mL, 1×) and dried over Na_2SO_4 to give a colorless liquid **1B** (4.8 g, 92%).

^{1}H NMR (300 MHz, $CDCl_3$), δ (ppm): 0.08 (s, 12H), 0.91 (s, 18H), 2.45 (s, 1H), 3.65 (s, 5H).

1,3-Bis(*tert*-butyldimethylsilyloxy)-2-propanol **1B** (2.0 g, 6.24 mmol) was dissolved in anhydrous DCM (12 mL) followed by DMAP (0.153 g, 1.25 mmol) added with an ice bath, and butyric anhydride (6.11 mL, 37.4 mmol) was added dropwise. The mixture was stirred for an hour at room temperature with N_2 protection and was heated to reflux overnight. The reaction was quenched by addition of water (~5 mL), and the excess of butyric anhydride was removed by pouring the mixture into saturated $NaHCO_3$ (100 mL) with vigorous stirring overnight. The product was extracted by ethyl acetate (20 mL, 3×) and washed with dilute HCl solution (1 M, 20 mL), water (20 mL), and brine (20 mL) and dried over Na_2SO_4. The filtrate was concentrated under vacuum and purified by silica column chromatography (10% ethyl acetate, 90% hexane, R_f = 0.7) to give a colorless oil **1C** (1.75 g, 72%).

^{1}H NMR (300 MHz, $CDCl_3$), δ (ppm): 0.06 (s, 12H), 0.89 (s, 18H), 0.96 (t, J = 7.5 Hz, 3H), 1.60−1.73 (m, 2H), 2.30 (t, J = 7.5 Hz, 2H), 3.69−3.70 (m, 4H), 4.89 (quin, J = 5.25 Hz, 1H).

TBDMS protected 2-butyryloxypropane-1,3-diol **1C** (1.75 g, 4.49 mmol) was dissolved in anhydrous THF (30 mL) at room temperature under N_2, and tBAF (12.6 mL, 1 M solution in THF) was added. The mixture was stirred for 2 h and was concentrated under vacuum. The product was purified by silica column chromatography (100% ethyl acetate) to give a colorless oil (0.51 g, 70%).

^{1}H NMR (300 MHz, DMSO-d_6), δ (ppm): 0.89 (t, J = 7.5 Hz, 3H), 1.51−1.58 (m, 2H), 2.28 (t, J = 7.5 Hz, 2H), 3.32−3.36 (m, 2H), 3.60−3.66 (m, 1H), 3.87−3.93 (m, 1H), 4.02−4.07 (m, 1H), 4.59 (t, J = 6 Hz, 1H), 4.83 (d, J = 6 Hz, 1H).

^{13}C NMR (300 MHz, DMSO-d_6), δ (ppm): 13.44 (s), 17.93 (s), 36.35 (s), 62.63 (s), 65.48 (s), 69.28 (s), 172.82 (s).

ESI-MS ([M + Na]$^+$): 185.0 (calcd: 162.0).

Synthesis of *N*-(1,3-Dihydroxypropan-2-yl)butanamide. Serinol (9.11 g, 100 mmol) and methyl butyrate (5.16 g, 50 mmol) were added into a 100 mL round-bottom flask, and the reagents were heated at 80 °C overnight under vacuum. The product was purified by silica column chromatography (10% MeOH, 90% DCM) to give a white solid (8.14 g, 88%).

^{1}H NMR (300 MHz, DMSO-d_6), δ (ppm): 0.84 (t, J = 7.5 Hz, 3H), 1.43−1.55 (m, 2H), 2.05 (t, J = 7.5 Hz, 2H), 3.38 (t, J = 9 Hz, 4H), 3.65−3.75 (m, 1H), 4.53 (t, J = 6 Hz, 2H), 7.38 (d, J = 9 Hz, 1H).

^{13}C NMR (300 MHz, DMSO-d_6), δ (ppm): 13.58 (s), 18.72 (s), 37.36 (s), 52.77 (s), 60.30 (s), 172.03 (s).

ESI-MS ([M + Na]$^+$): 184.2 (calcd: 161.2).

Synthesis of Monomer with 2-Amide-Propyl Groups in the Pendant Group. 4-Aminobutyric acid (10.3 g, 99.6 mmol) was dissolved in anhydrous MeOH (120 mL), and thionyl chloride (18.08 mL, 249 mmol) was added dropwise via an additional funnel at 0 °C. The ice bath was removed after 30 min, and the reaction mixture was stirred at room temperature overnight. Solvent and excess of thionyl chloride were removed under vacuum to give a white solid **3A**. The crude product was used without further purification.

In a round-bottom flask equipped with a magnetic stir bar, methyl 4-aminobutyrate (16.6 g, 96 mmol) (**3A**) and a mixture of water (15 mL) and dioxane (45 mL) were added. TEA (24.3 g, 240 mmol) was added at 0 °C. Butyric anhydride (38 g, 240 mmol) in a mixture of water (10 mL) and dioxane (30 mL) was added into the round-bottom flask dropwise, and the reaction was performed at room temperature overnight open to the atmosphere. Solvents were removed under vacuum, and the residue was poured into saturated $NaHCO_3$ solution (500 mL) overnight with vigorous stirring. The product was extracted with ethyl acetate (60 mL, 3×), washed with saturated $NaHCO_3$ (50 mL, 2×) and brine (50 mL, 1×), and dried over Na_2SO_4. The organic phase was concentrated under vacuum to give a white solid **3B** (16.33 g, 91%).

^{1}H NMR (300 MHz, $CDCl_3$), δ (ppm): 0.95 (t, J = 7.5 Hz, 3H), 1.60−1.72 (m, 2H), 1.85 (quin, J = 6.75 Hz, 2H), 2.14 (t, J = 7.5 Hz, 2H), 2.38 (t, J = 7.5 Hz, 2H), 2.30 (q, J = 7 Hz, 2H), 3.68 (s, 3H), 5.70 (br s, 1H).

Methyl 4-butanamidobutanoate (**3B**) (13.0 g, 69.5 mmol) and serinol (9.4 g, 103.2 mmol) were added into a 200 mL round-bottom flask, and the mixture was stirred at 80 °C under vacuum overnight. After reaction, the monomer was purified by silica column chromatography (20% MeOH, 80% DCM, R_f = 0.3) to give a white solid (17.42 g, 81%).

^{1}H NMR (300 MHz, DMSO-d_6), δ (ppm): 0.84 (t, J = 7.5 Hz, 3H), 1.44−1.56 (m, 2H), 1.59 (quin, J = 7.5 Hz, 2H), 2.02 (t, J = 7.5 Hz, 2H), 2.07 (t, J = 7.5 Hz, 2H), 3.01 (q, J = 6 Hz, 2H), 3.38 (t, J = 6 Hz, 4H), 3.64−3.75 (m, 1H), 4.55 (t, J = 6 Hz, 2H), 7.44 (d, J = 9 Hz, 1H), 7.72 (t, J = 9 Hz, 1H).

^{13}C NMR (300 MHz, DMSO-d_6), δ (ppm): 13.63 (s), 18.69 (s), 25.59 (s), 32.97 (s), 37.41 (s), 38.05 (s), 52.82 (s), 60.26 (s), 171.77 (s), 171 89 (s).

ESI-MS ([M + Na]$^+$): 269.2 (calcd: 246.2).

Synthesis of Polyesters. The polyesters were obtained by step-growth polymerization of ester-functionalized diol and amide-functionalized diols and succinic acid. As an illustrative example, the synthesis of P(1EP) is as follows: 2-butyryloxypropane-1,3-diol (0.50 g, 3.08 mmol), succinic acid (0.364 g, 3.08 mmol), and DPTS (0.36 g, 1.23 mmol) were added into a 100 mL round-bottom flask. The flask was evacuated and backfilled with N_2 for three times. Anhydrous DCM (6 mL) was added into the flask via a syringe under N_2 protection. DIC (1.5 mL, 9.5 mmol) was added dropwise into the reaction mixture at 0 °C. The mixture was stirred at room temperature for 48 h. Polymer was purified by dialyzing against MeOH and dried under vacuum to give a viscous polymer.

P(1EP). ^{1}H NMR (300 MHz, DMSO-d_6), δ (ppm): 0.87 (t, J = 7.5 Hz, 3H), 1.49−1.59 (m, 2H), 2.27 (t, J = 7.5 Hz, 2H), 2.56 (s, 4H), 4.1−4.25 (m, 4H), 5.17 (quin, J = 4.5 Hz, 1H).

P(1AP). ^{1}H NMR (300 MHz, DMSO-d_6), δ (ppm): 0.84 (t, J = 7.5 Hz, 3H), 1.44−1.56 (m, 2H), 2.05 (t, J = 7.5 Hz, 2H), 2.56 (s, 4H), 3.95−4.09 (m, 4H), 4.18−4.24 (m, 1H), 7.88 (d, J = 9 Hz, 1H).

P(2AP). ^{1}H NMR (300 MHz, DMSO-d_6), δ (ppm): 0.83 (t, J = 7.5 Hz, 3H), 1.43−1.55 (m, 2H), 1.59 (quin, J = 6.75 Hz, 2H), 2.01 (t, J = 7.5 Hz, 2H), 2.07 (t, J = 7.5 Hz, 2H), 2.56 (s, 4H), 3.01 (q, J = 6 Hz, 2H), 3.96−4.09 (m, 4H), 4.19 (quin, J = 6 Hz, 1H), 7.76 (t, J = 4.5 Hz, 1H), 7.94 (d, J = 9 Hz, 1H).

Temperature Dependence of IR Absorption. FT-IR samples were prepared by casting thin film of polymers on potassium bromide (KBr) pellets from 5% (w/w) polymer solution (DCM was used for P(1EP), and MeOH was used for P(1AP) and P(2AP)). Samples were kept in ambient environment for 12 h to remove the majority of solvent and then kept into a high vacuum oven at 70 °C overnight to remove the residual solvent and moisture. An FT-IR spectrophotometer (Thermo Nicolet 380) with a temperature chamber was used to monitor the change of the spectra over temperature. Temperature was raised from 40 to 200 °C with an interval of 20 °C. Samples were kept isothermal for 5 min at each temperature before testing. 32 scans and a resolution of 2 cm^{-1} were used in the test. Peak fitting of the bonded and "free" N−H stretching peaks was done with OriginPro 9.0, and the integration of each peak was obtained.

Mechanical Properties. Thin films of polymers were prepared by a vacuum compression machine (TMP technical Machine Products Corp.) and cut into specimens. Mechanical properties of the polymers were tested by tensile test at 21 °C using an Instron 5567. The speed of crosshead was set as 3 mm/min. Dimensions of samples are 20.0 mm in length, 2.0 mm in width, and 0.5 mm in thickness. Reported data were based on triplet results of each sample under the same testing condition. P(2AP) fractured every time between clamps before stretching due to its brittleness, so cardboard was used to cover specimen ends when clamped. Even so, the sample fractured inside or by the edge of the clamps during stretching, resulting in quite small strain at the break. The ultimate strength and strain at break were

DOI: 10.1021/acs.macromol.8b01781
Macromolecules 2018, 51, 9294−9305

Scheme 1. Synthetic Routes for Functionalized Diols and Polyesters[a]

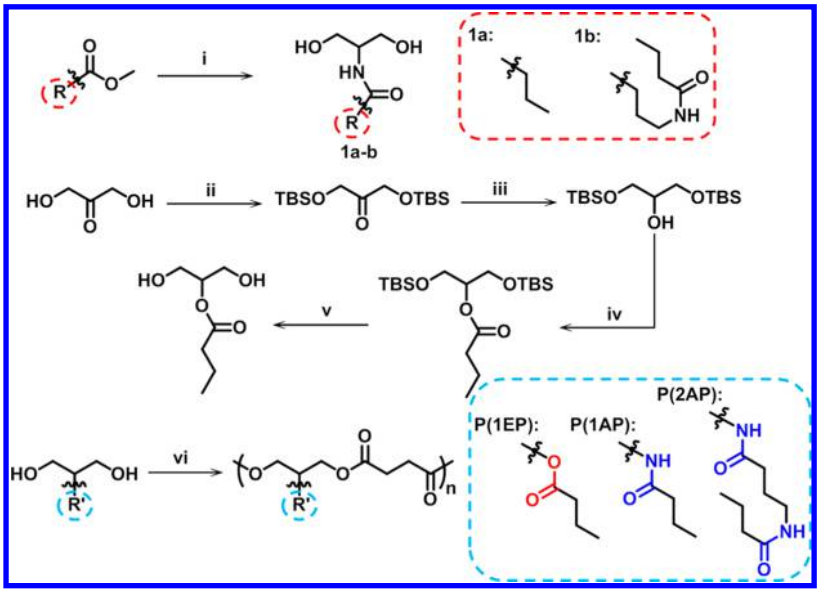

[a]Reagents and conditions: (i) serinol, 80 °C, overnight; (ii) *tert*-butyldimethylsilyl chloride, imidazole, THF, RT, 12 h; (iii) sodium borohydride, 0 °C, 1 h; (iv) butyric anhydride, DMAP, CH_2Cl_2, 0 °C to RT, 1 h, 50 °C, 1 h; (v): TBAF solution, 1.0 M in THF, THF, RT, 2 h; (vi) succinic acid, DIC, DPTS, DCM, 0 °C to RT, 48 h.

expected to be higher if dumbbell-shaped specimens were used, but the dumbbell-shaped specimens were not achievable with P(2AP) because the brittle material fractured when cut into a dumbbell shape. Handling instructions for these hygroscopic materials are provided in the Supporting Information.

Rheological Properties. Storage modulus (G'), loss modulus (G''), and complex viscosity (η^*) were measured with a TA Instruments ARES-G2 rheometer with 8.0 mm parallel stainless steel plates. For polymer P(1AP) and P(2AP), thin films (1 mm thickness and 8 mm diameter) were fabricated by compression molding and placed between the plates for testing. P(1EP) was too soft to be molded into a film; thus, it was loaded between the plates directly. All samples were loaded at T_g + 70 °C. Before each test, a strain sweep at a frequency of 1 rad/s and strains varied between 0.1 and 100% was used to determine the linear viscoelastic (LVE) region of the samples. Each sample was run at different temperatures with a strain value within the LVE region and a frequency range from 0.1 to 100 rad/s. A master curve with a reference temperature of T_g + 50 °C was obtained using time-temperature superposition for each sample, where the shift factors for G' and G'' were calculated by TRIOS software. Handling instructions for these hygroscopic materials are provided in the Supporting Information.

Hygroscopic Properties. P(1AP) and P(2AP) absorb water from the ambient environment due to amide groups. A chamber with constant relative humidity (60%) was built to provide moisture to study the hygroscopic property. Polymer specimens with dimensions of 3 mm × 3 mm × 0.5 mm and 5 mm × 5 mm × 0.5 mm were incubated for a specific time for TGA and DSC studies. The weight of the absorbed water was performed on TGA where temperature was raised from 20 to 400 °C with a heating rate of 10 °C/min. The decrease of T_g with incubating time was monitored by DSC with a scanning range of −50 to 50 °C and a scanning rate of 10 °C/min.

RESULTS AND DISCUSSION

Polymer Synthesis and Characterizations. Gokhale et al.[30] reported the synthesis of a library of "peptide-like" polyesters by carbodiimide coupling of functionalized diols and diacids under mild reaction conditions. The functionalized diols are derived by functionalizing diethanolamine by a transamidation reaction with various methyl esters. This provides a tertiary amide substituted diol, and the resulting polyesters are relatively of low modulus due to the absence of hydrogen bonding donor atoms. However, if the tertiary amide is substituted with a secondary amide, it will introduce hydrogen bonds and can strengthen the material. In this work, we explored this aspect by using serinol, a diol with primary amine groups, instead of diethanolamine, to make functionalized diols. Three different polyesters were designed for this study. Two of them were synthesized by transamidation of serinol, and methyl esters had either one secondary amide-propyl group or two secondary amide-propyl groups. As a control, a diol containing an ester group (instead of the secondary amide) was made. Synthetic routes are illustrated in Scheme 1, and ^{1}H NMR spectra of the three polyesters are presented in Figure 1.

Polymers with similar M_w were synthesized and characterized (Table 1). Molecular mass distributions (dispersity, $Đ$) of the polymers are ∼2, which is the theoretical $Đ$ value for step growth polymerization. P(1EP) has the lowest T_g of −18 °C and is in its rubbery state at ambient conditions. The substitution of an amide group in P(1AP) for the ester group in the side-chain of P(1EP) increased the T_g to 28 °C for P(1AP) as a result of stronger supramolecular bonding between amide groups. Ester groups form dipole-dipole interactions between the carbonyl groups[34,35] but do not form hydrogen bonds because of the unavailability of covalently bonded hydrogen to highly electronegative atoms like N, O, and F. The higher polarity of amide groups enables formation of strong hydrogen bonds between the carbonyl oxygen and the hydrogen of the N−H group.[36] As a result, the amide groups in P(1AP) are more effective than the dipolar interactions of the ester groups in P(1EP) in suppressing segmental motion, which increases T_g. The increase of T_g due to hydrogen bonding interaction has been reported by several groups.[37,28,27,32] Lewis and co-workers observed that T_g increased almost linearly with concentration of hydrogen bonding groups in copolymers of which one component has

DOI: 10.1021/acs.macromol.8b01781
Macromolecules 2018, 51, 9294−9305

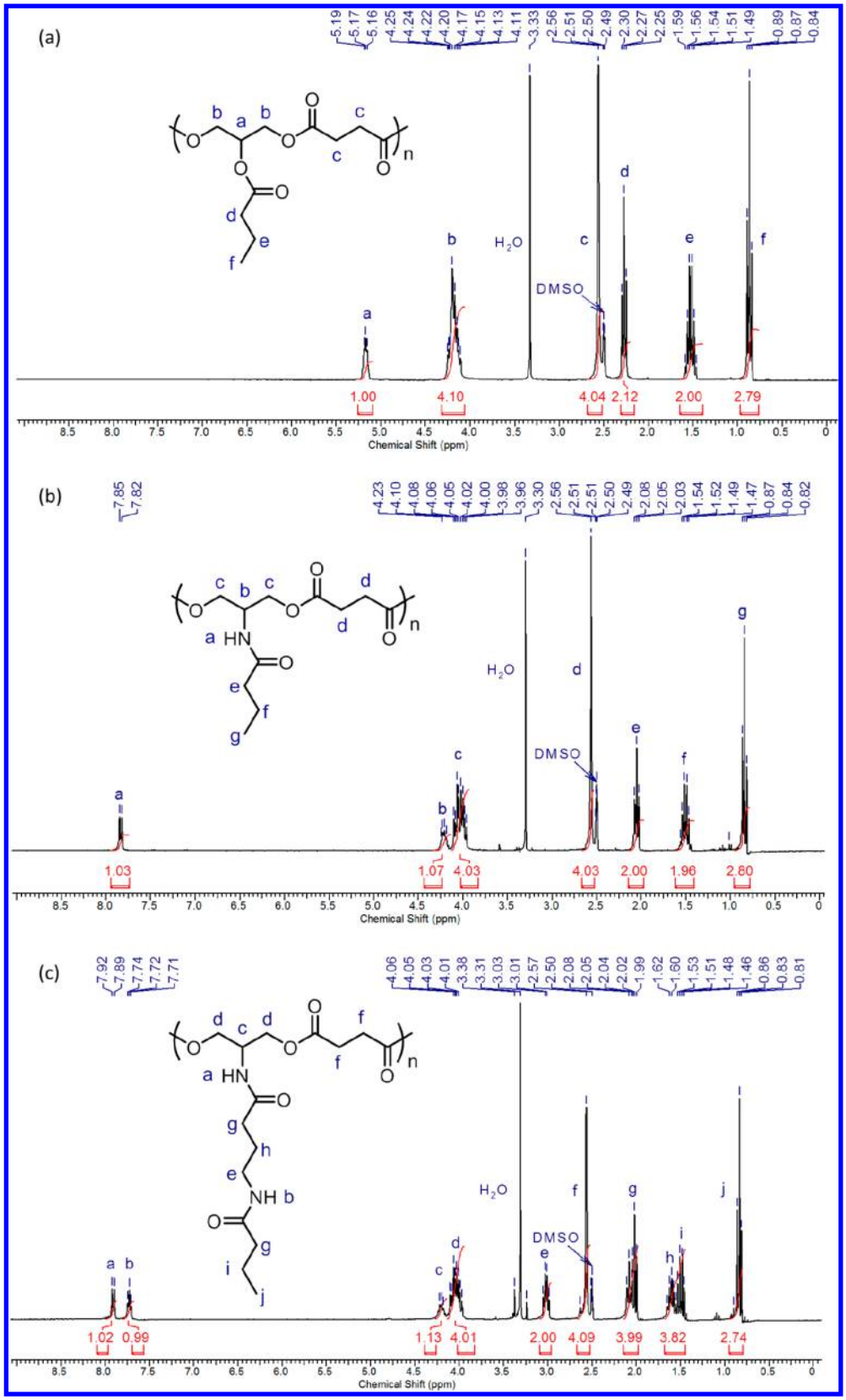

Figure 1. ^{1}H NMR spectra of (a) P(1EP), (b) P(1AP), and (c) P(2AP) in DMSO-d_6.

either acrylic acid, carboxy ethyl acrylate, or aminopyridine side-chain.[28] It was expected that P(2AP) would have a significantly higher T_g than P(1AP) because the amide group concentration with P(2AP) is twice as that of P(1AP). However, the T_g of P(2AP) is only 6 °C higher than that of P(1AP), and it is hypothesized that the inherent flexibility and the longer length of the secondary amide containing side-chain of P(2AP) play roles in decreasing T_g. Flexible polymers tend

DOI: 10.1021/acs.macromol.8b01781
Macromolecules 2018, 51, 9294−9305

Table 1. Characterization of Polyesters with Different Pendant Groups

sample	M_n[a] (kDa)	M_w[a] (kDa)	$Đ$[a]	T_g[b] (°C)
P(1EP)	51.7	100.0	1.93	−18
P(1AP)	51.3	97.7	1.90	28
P(2AP)	48.4	89.3	1.85	34

[a]Determined by GPC with DMF as eluent. [b]Determined by DSC with heating rate of 10 °C/min.

to have low T_g, while formation of hydrogen bonds limit chain mobility, which results in increase of T_g. The combined effects of chain flexibility and increased hydrogen bonding lead to a 6 °C higher T_g in P(2AP) compared to P(1AP). More evidence of the side-chain flexibility of P(2AP) is shown in the rheology study.

Temperature-Dependent IR Absorption Spectrosopy. The strength of hydrogen bonds is highly dependent on temperature.[38,39] The FT-IR spectrum of P(1EP) did not change with tempeprature (Figure S1), while those of P(1AP) and P(2AP) varied significantly with increase of temperature (Figure S1). For P(1AP) and P(2AP), bands of N−H stretching peaks (~3300 cm^{-1}) and amide I/II modes (~1650 and 1550 cm^{-1}) were analyzed in detail to study the extent of hydrogen bonding in the system.[40] All spectra were normalized against the asymmetric C−H stretching peak (~2964 cm^{-1}) whose intensity did not change with increase of temperautre, and peak fitting was done to the N−H stretching region with Gaussian band shapes using OriginPro 9.0. As an example, major infrared peaks of P(1AP) are assigned in Table 2.

Table 2. Assignments of Infrared Peaks of P(1AP)[40]

peak position (cm^{-1})	description
3378	free N−H stretching
3280	hydrogen bonded N−H stretching
3200	amide B mode
3069	overtone of N−H stretching vibration
2964	asymmetric CH_2 stretching
2876	symmetric CH_2 stretching
1739	C═O stretching
1652	amide I mode
1544	amide II mode

Figure 2a shows evidence for intense hydrogen bonded N−H stretching peaks (~3280 cm^{-1}) in P(1AP) and P(2AP), while the "free" N−H peak (~3378 cm^{-1}) is a small shoulder of the main peak. With increase in temperature, the intensity and area of the H-bonded N−H stretching peaks decrease, and the peak position shifts to higher wavenumber (Figure 2 and Figure S2b). They indicate the decrease of the averaged hydrogen bond strength.[40] However, the area of the "free" N−H stretching peak remains almost constant (Figure 2b). It has been pointed out that absorption coefficients of hydrogen bonded and "free" N−H streching are dependent on temperautre, with a 3.2:1 ratio of absorption coeffeicents between the hydrogen bonded N−H and free N−H bonds based on three model polyurethanes.[40,41] Therefore, the nonlinear reduction of the hydrogen bonded N−H stretching peak area with increase of temperature is mainly due to the significant decrease of the absorption coefficient of the hydrogen bonded N−H mode.[40] Thus, the increase of temperature has a greater influence on the reduction of the hydrogen bonded N−H stretching peak than it has on the "free" N−H stretching peak.

In the FT-IR spectrum of P(1AP), the peak at 1650 cm^{-1} is assigned as the amide I mode with major contribution from C═O stretching (main peak: hydrogen bonded C═O stretching; shoulder of the peak: "free" C═O stretching). The main peak shifts from 1652 to 1664 cm^{-1}, and the peak intensity decreases with increase of temperature. The behavior of amide I mode with temperature is consistent with that of N−H stretching vibration because of the correspondence between N−H and C═O groups.[40] The peak at 1550 cm^{-1} is assigned as amide II mode which originates from N−H in-plane deformation vibration. The peak shifts from 1544 to 1522 cm^{-1}, and the intensity decreases with the increase of temperature, indicating the weakening of hydrogen bonds. Similar trends of changes with increase of temperature were observed from P(2AP) (Figure S2a). The intensities of the N−H stretching band as well as amide I and amide II modes of P(2AP) are stronger than those of P(1AP) due to the higher mol % of amide groups. As shown below, the higher concentration of secondary amide groups in P(2AP) compared to P(1AP), will have a corresponding influence on the mechanincal properties as well as the hydrophilic and hygroscopic nature of the polymers.

Mechanical Properties. The hydrogen bonded secondary amide groups are expected to serve as supramolecular cross-links and reinforce the material. Tensile tests were performed to evaluate structure-mechanical property relationships of P(1AP) and P(2AP). (P(1EP) is a sticky liquid and is too soft to be used for a mechanical test at room temperature.) Engineering stress versus strain curves of P(1AP) and P(2AP) are plotted in Figure 3, and the mechanical properties are summarized in Table 3. The results show that P(1AP) is a tough material with strain at break exceeding 400%. With P(1AP), after yielding it was observed that necking appeared near the clamped parts of the specimen (stress concentrated spots), and the material turned white and became opaque due to formation of crazing (Figure S3). During stretching, crazing still bears load and continues to dissipate energy before formation of a crack, which leads to failure of the sample.[42] Formation of crazes is regarded as a toughening mechanism.[43]

The occurrence of yielding indicates the beginning of plastic deformation. The elongated material tended to retract back to its original shape after fracture due to dynamic cross-linking by hydrogen bonding interactions and rubber elasticity. Tensile measurements of P(2AP) showed that the material is stiffer and more brittle than P(1AP) with a Young's modulus 12 times higher than for P(1AP) while a strain at break 1/800 of P(1AP). Tensile results are consistent with the expectation that the extra hydrogen bonding amide-propyl group will lead to increased supramolecular cross-links and a stiffer, stronger, and more brittle material.[44−46] In addition, as shown by the mechanical tests, introduction of an extra amide-propyl group raised the T_g of P(2AP) and resulted in P(2AP) exhibiting greater glassy behavior than P(1AP).

Rheological Properties. To weaken the effects of hydrogen bonds and highlight the role of side-chain flexibility, the materials were characterized at higher temperatures. Because the polymers were too weak for tensile testing at high temperature (higher than T_g), rheological analysis was done instead to observe the interplay of the hydrogen bonding and chain flexibility on viscoelasticity of the materials. Figure 4

DOI: 10.1021/acs.macromol.8b01781
Macromolecules 2018, 51, 9294−9305

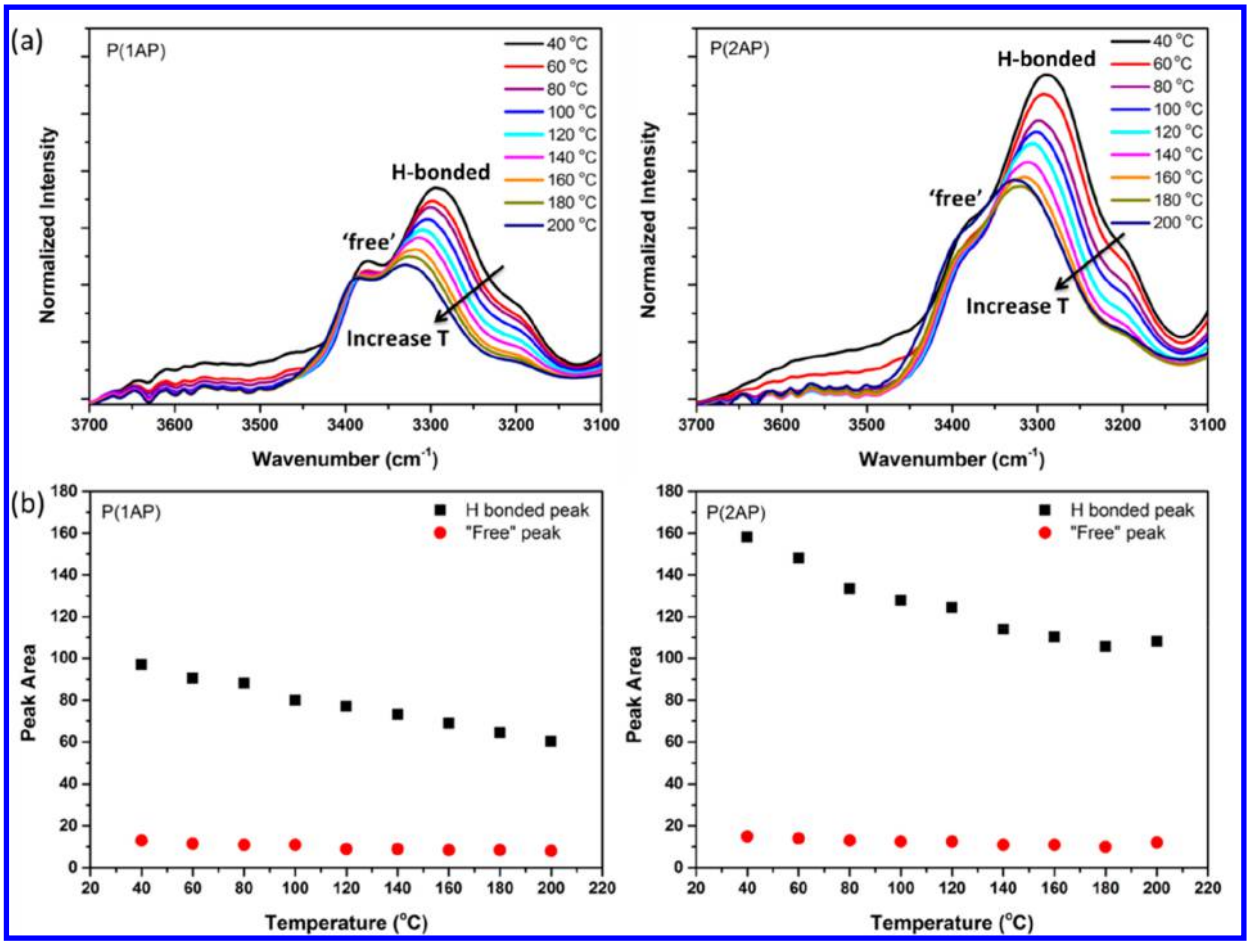

Figure 2. (a) Expanded FT-IR spectra of N−H stretching band of P(1AP) and P(2AP) at various temperatures. Temperature increases toward the direction of the arrowhead. (b) Peak areas of H-bonded and "free" N−H stretching peak of P(1AP) and P(2AP) at different temperatures.

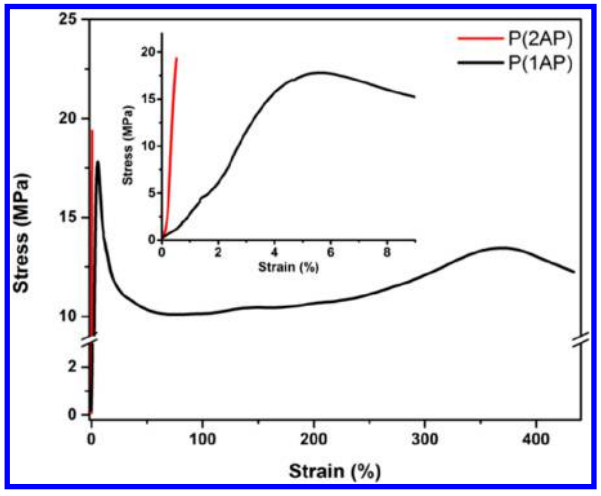

Figure 3. Engineering stress versus strain curves of P(1AP) (black) and P(2AP) (red).

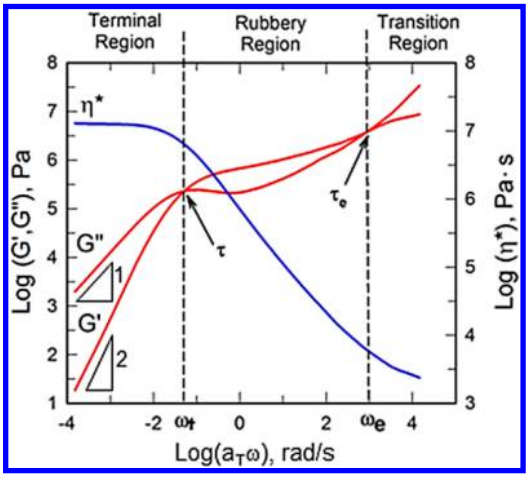

Figure 4. Schematic of the idealized LVE behavior of a high molecular mass amorphous polymer above T_g.

is a schematic of the idealized linear viscoelastic behavior of a high molar mass amorphous polymer above its T_g. The G' and

Table 3. Summary of Mechanical Properties with P(1AP) and P(2AP)

sample	stress at break (MPa)	strain at break (%)	Young's modulus (GPa)	yield stress (MPa)	strain at yield point (%)
P(1AP)	11.6 ± 1.20	423 ± 11.2	0.470 ± 0.0600	16.3 ± 2.20	6.87 ± 1.13
P(2AP)	16.4 ± 2.87	0.530 ± 0.0800	5.53 ± 0.830	N/A	N/A

DOI: 10.1021/acs.macromol.8b01781
Macromolecules 2018, 51, 9294−9305

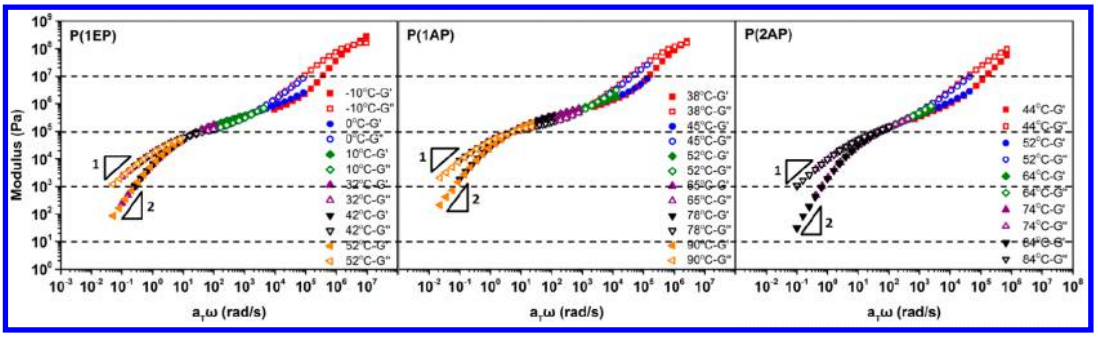

Figure 5. Comparison of the G' and G'' master curves for the three polymers at a reference temperature of $T_r = T_g + 50$ °C.

Table 4. Rheological Properties of the Three Polymers According to TTS at $T_r = T_g + 50$ °C and Activation Energy for Flow Based on the Arrhenius Equation

sample	ω_t[a] (rad/s)	ω_e[a] (rad/s)	τ[a] (s)	τ_e[a] (s)	G_e[a] (Pa)	η^*_0[b] (Pas)	E_a[c] (kJ/mol)
P(1EP)	1.54×10^1	2.12×10^3	4.08×10^{-1}	2.9×10^{-3}	4.80×10^5	2.33×10^4	45.3
P(1AP)	5.19×10^0	1.89×10^3	1.21×10^0	3.3×10^{-3}	8.44×10^5	9.42×10^4	60.6
P(2AP)	1.03×10^2	2.50×10^2	6.1×10^{-2}	2.5×10^{-2}	2.02×10^5	1.08×10^4	67.4

[a]Determined from Figure 5. [b]Determined from Figure 7. [c]Determined from Figure S7.

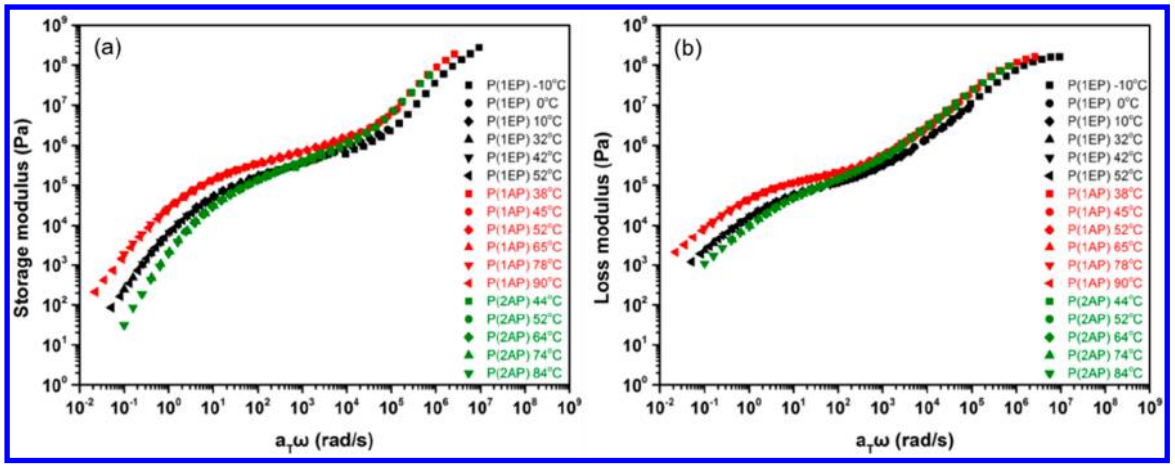

Figure 6. Comparison of the (a) storage moduli and (b) loss moduli for the three polymers at a common reference temperature of $T_r = T_g + 50$ °C.

G'' data cross at two distinct frequencies, ω_t and ω_e, which are the onset of terminal (i.e., viscous flow) behavior and the reciprocal of Rouse time of a strand between two entanglements, respectively. In the terminal region, polymer chains have enough time to relax and flow freely. The Rouse time is the longest relaxation time for an unentangled chain, while in an entangled network, the Rouse model is only applicable where $\omega > \omega_e$. The two dotted lines in Figure 4 indicate the demarcation from terminal to rubbery plateau behavior at the lower frequency and from rubbery to the transition region at higher frequency. The material properties that can be extracted from the data in Figure 4 include the Rouse relaxation time for the entangled strands (τ_e), the terminal relaxation time (τ), and the plateau modulus (G_e), which is the value of G' at $\omega = \omega_e$.[47] The molecular mass between entanglements or supramolecular cross-links (M_e) can be obtained from the equation

$$M_e = \rho RT/G_e$$

where ρ is the mass density of the polymer, R is the gas constant, and T is the absolute temperature.

To study rheological behaviors of the three polymers in a wider frequency range, the principle of time-temperature superposition[48] (TTS) was used to prepare linear viscoelastic (LVE) master curves of G' and G'' versus reduced frequency ($a_T\omega$) from the LVE data measured at 5−6 temperatures between −10 and 90 °C. The results are shown in Figure 5 at a reference temperature of $T_r = T_g + 50$ °C for each polymer to remove the influence of T_g. Theoretically, TTS is valid for a homogeneous system where all relaxation modes have the same temperature dependence.[49] It fails in some complex systems, like some polymer blends and branched polymers, and in some polymers with temperature dependent supramolecular interactions. TTS works well for the current polymers although these polymers have supramolecular interactions, i.e., dipole-dipole interaction and hydrogen bonding, and the data points collected from the range of temperatures were superposed for each polymer. The effects of temperature over the relatively narrow range of temperatures used in this study did not significantly affect the relaxation times of the polymers. Previous reports pointed out that TTS was applicable to systems with weak hydrogen bonding interactions such as systems with urazole groups, acrylamido-

DOI: 10.1021/acs.macromol.8b01781
Macromolecules 2018, 51, 9294−9305

pyridines, and acrylic acid moieties but failed in systems with stronger interactions such as trimeric and quadruple hydrogen bonding groups.[29]

The LVE response at low frequency, which corresponds to the data at higher temperatures, shows terminal behavior of the polymer melt. That is confirmed by the scaling of the moduli with frequency, $G' \propto \omega^2$ and $G'' \propto \omega$, which indicates that all three polymer melts are thermally simple in the terminal region. The terminal (longest) relaxation time of the polymers which corresponds to translation of chains was calculated from the crossover frequency, $\tau = 2\pi/\omega_b$ where $G' = G''$ ($\tan \delta = 1.00$), and the values for the three polymers are listed in Table 4. P(2AP) has the shortest τ, which is 6.1×10^{-2} s, and P(1AP) has the longest τ of 1.21×10^{0} s. P(1EP) has an intermediate τ value of 4.08×10^{-1} s.

From the LVE master curves in Figure 5, the terminal relaxation time (τ) increased by 3 times when the ester side group (P(1EP)) was replaced with an amide group (P(1AP)). The increase in τ is due to the hydrogen bonds in the latter polymer, which act as temporal cross-links that suppress translation of the polymer chains. Besides, P(1EP) showed lower moduli than P(1AP) at specific frequencies as well as lower plateau modulus and complex viscosity (Figures 6 and 7).

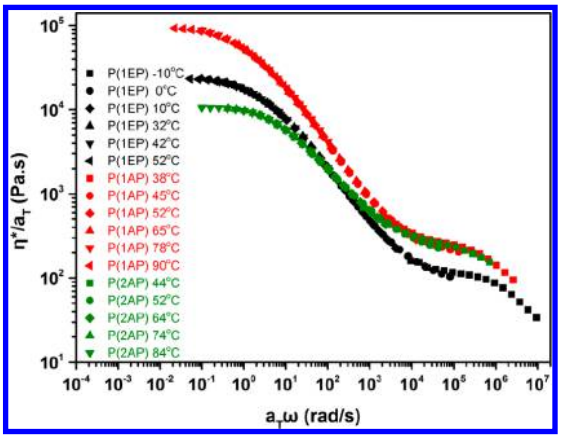

Figure 7. Comparison of the complex viscosity for the three polymers at a common reference temperature of $T_r = T_g + 50$ °C.

Surprisingly, the addition of a secondary amide group in the side-chain did not further increase τ. On the contrary, P(2AP) had the shortest terminal relaxation time. That difference cannot be fully explained by the differences in the M_w of the two polymers (M_w of P(1AP): 97.7 kDa; M_w of P(2AP): 89.3 kDa). In general, for high-M_w linear polymers, $\tau \propto M_w^{3.4}$. τ for P(1AP) is 1.21 s (Table 4), and that for P(1AP) with the same M_w as P(2AP) is calculated to be 0.891 s (Supporting Information). However, τ for P(2AP) is 0.061 s, which is 14 times smaller than that of P(1AP) with the same M_w.

The plateau modulus (G_e) for P(1AP) is 4 times that of P(2AP). Based on the above equation and by measuring the density of P(1AP) and P(2AP) ($\rho_{P(1AP)} = 1.24$, $\rho_{P(2AP)} = 1.19$, measured by dividing mass by volume), it is calculated that M_e of P(2AP) is 4 times as high as that of P(1AP). In addition, τ_e for P(2AP) is 7.5 times as high as that for P(1AP). Thus, P(1AP) has a higher physical cross-link density than P(2AP). As a matter of fact, P(2AP) has even lower relaxation time and plateau modulus than P(1EP), which theoretically does not participate in hydrogen bond formation. It indicates that at higher temperature where the strength of hydrogen bonds is decreased, the effect of side-chain flexibility plays a significant role. The energy of rotation of the backbone decreases and free volume increases because the longer flexible side-chains function as "internal diluents".[31] In polyvinyls it is observed that the more methylene groups the side-chain has, the lower is the T_g, as long as crystallization does not occur.[50−53] P(2AP) has the longest inherently flexible side-chain, and at higher temperature where hydrogen bonds strengths are weakened, the roles of chain flexibility and side-chain length are more dominant, and thus the material shows the shortest terminal relaxation time and the lowest G_e.

In rheological studies, the viscoelastic behaviors of polymers are normally compared at a fixed temperature interval above T_g ($T_r = T_g + T$) to remove the influence of T_g. However, this does not provide a complete picture as the strength of the hydrogen bonds is influenced by temperature. The strength of a hydrogen bond in P(2AP) will be weaker when compared to P(1AP) as the former is performed at 84 °C ($T_r = T_g + 50$ °C), while the latter is performed at 78 °C. To remove the influence of temperature on the strength of the hydrogen bonds, the LVE behavior of the three polyesters was also compared at a common temperature of 52 °C as shown in Figure S4. G_e for each polymer remains the same when the reference temperature changes. P(1AP) has the highest τ of 154 s and P(1EP) has the smallest τ of 0.0322 s because of its low T_g. P(2AP) shows an intermediate τ of 21.6 s. τ_e for P(1AP) and P(2AP) are 0.421 and 13.4 s, respectively. In this comparison, P(2AP) has a higher terminal relaxation time than P(1EP) but still has a shorter terminal relaxation time and lower physical cross-link density than P(1AP), even though P(2AP) may have a greater glassy contribution to its LVE behavior than P(1AP). The comparison at a constant temperature, however, is consistent with the weakening of the amide hydrogen bonds, such that the flexibility of the longer side-chain in P(2AP) at 52 °C produces a lower terminal relaxation time.

The $G'(\omega)$, $G''(\omega)$, and $\eta^*(\omega)$ master curves for all of the polymers at the reference temperature of $T_r = T_g + 50$ °C are plotted in Figures 6 and 7. In Figure 6, both G' (Figure 6a) and G'' (Figure 6b) of P(1AP) and P(2AP) overlap at high frequency, where the materials enter into glassy state. P(2AP), however, exhibits a shorter rubbery region, which indicates that the chemical structures of the two materials have a significant influence on the motion of polymer chains. In the complex viscosity versus frequency plot (Figure 7), a constant, zero-shear rate viscosity is observed at low frequency. P(1AP) and P(2AP) show the highest and lowest zero-shear viscosity: 9.42×10^4 Pa·s and 1.08×10^4 Pa·s (Table 4), respectively. Viscosity data also confirmed the greater diluting effect of longer flexible side-chain. With the increase of frequency, complex viscosity decreases and the viscosity difference between P(1AP) and P(2AP) decreases.

Master curves of $G'(\omega)$, $G''(\omega)$, and $\eta^*(\omega)$ for the three polyesters are compared at $T_r = 52$ °C as well (Figures S5 and S6). In the terminal region, G' and G'' of P(2AP) are lower than those of P(1AP). In addition, P(2AP) shows a lower zero shear viscosity than P(1AP). These observations are in keeping with the study at $T_r = T_g + 50$ °C. With the frequency increasing, G', G'', and η^* of P(2AP) surpass those of P(1AP) due to the influence of T_g (P(2AP) enters into the glassy region earlier). P(1EP) shows the lowest G', G'', and η^* at all frequencies due to its low T_g. The rheological properties of the three polyesters at $T_r = 52$ °C are summarized in Table S1.

DOI: 10.1021/acs.macromol.8b01781
Macromolecules 2018, 51, 9294−9305

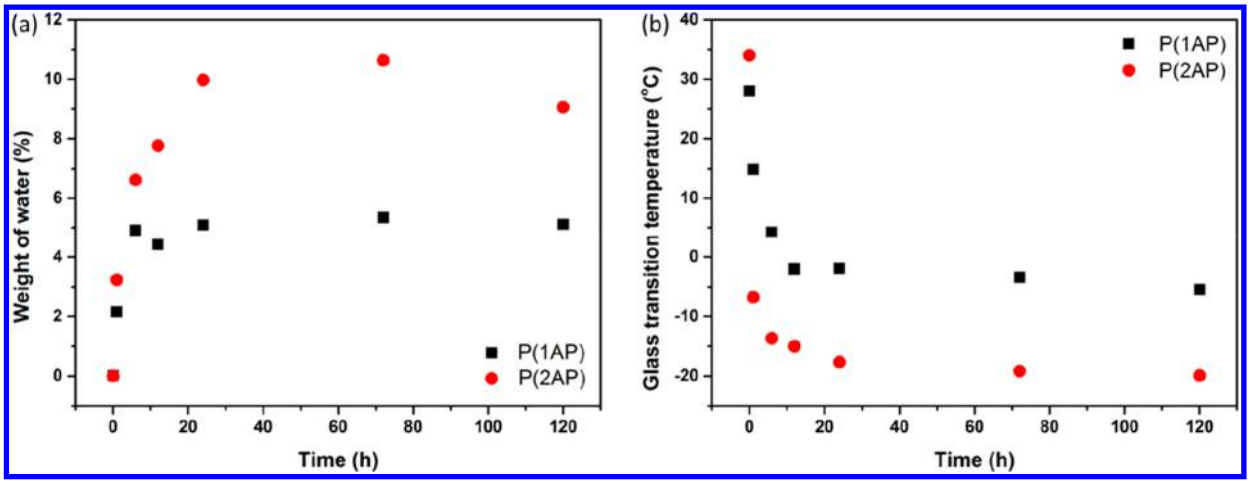

Figure 8. (a) Amount of water absorbed by P(1AP) and P(2AP) at room temperature and 60% relative humidity determined from TGA. (b) Change of T_g of P(1AP) and P(2AP) determined from DSC.

The activation energy (E_a) for flow can be calculated from the Arrhenius equation (Figure S7) using shift factors obtained from TTS. The activation energy reflects the restriction of viscous flow of a material.[54] P(2AP) and P(1EP) have the highest and lowest E_a of 67.4 and 45.3 kJ/mol, respectively (Table 4). It shows that P(2AP) with two amide groups in the side-chain has to overcome a higher energy barrier to attain viscous flow compared to P(1AP) with one amide group. The viscous flow of P(2AP) requires a cooperative dissociation of two hydrogen bonds, whereas P(1AP) can relax with dissociation of one hydrogen bond. Besides, the activation energy indicates how fast the viscosity and polymer structure change with temperature.[54,55] The sensitivity of polymer properties such as modulus and viscosity to temperature is high when the E_a value is large. The increase of E_a with hydrogen bond concentration and the temperature dependence of hydrogen bond strength have been observed in several previous reports.[29,56,57] In this work, P(2AP) has the largest E_a because of the highest concentration of hydrogen bonds, and it exhibits the strongest competition between hydrogen bonding interactions and diluting effect of the long flexible side-chain on the polymer properties.

The mechanical and rheological behaviors of P(2AP) could be advantageous. If all the hydrogen bonds persisted at higher temperature, the material would be difficult to process due to the high viscosity. However, the weakening of hydrogen bonds at higher temperature and the flowability introduced by side-chain flexibility make processing easier. The addition of the second amide group in the side-chain improves processability at higher temperature yet gives better properties at room temperature.

Hygroscopic Properties. Because of the existence of amide groups, both P(1AP) and P(2AP) can absorb water molecules from the ambient environment. After keeping these polymers in a humidifier with 60% relative humidity for a specific time, the amounts of water absorbed by P(1AP) and P(2AP) were determined from TGA, and the change of T_g with the two polymers was monitored by DSC (Figure 8). TGA data showed that for both materials the initial water absorption rates were high. P(2AP) had a higher water absorption rate than P(1AP) and absorbed twice as much water as P(1AP). DSC data show that the T_g decreases dramatically with exposure time during the initial phase and then becomes constant. Hydrogen bonds formed between water molecules and amide groups weaken molecular interaction among polymer chains. Water molecules function as plasticizers and increase the polymer free volume and molecular mobility, which reduces the T_g.[58,59] After 1 h exposure of P(2AP) to 60% humidity, there were two thermal transitions at 33 and −6 °C (Figure S8). It is possible that the exposure time is not long enough for water molecules to diffuse in to the sample homogeneously and that the hydrated surface gives a low T_g, while the bulk remains dry. After 6 h exposure, there was only one thermal transition indicating the homogeneous wetting of the whole polymer. Once hydrated, T_g of P(2AP) was lower than that of P(1AP). P(2AP) absorbed more water molecules, and the longer side-chain of P(2AP) has a greater "dilution" effect. Because P(1AP) and P(2AP) can absorb moisture from the ambient environment, samples for mechanical and rheological analysis were run right after vacuum compression molding. After the run, TGA was used to confirm there was no water absorbed by samples in such short time. The experimental details for minimizing moisture absorption by the polymers before characterizations are provided in the Supporting Information. The hydrophilicity of the three materials was determined by static water contact angle measurement over a period of 2 min. It shows that P(2AP) and P(1EP) are the most hydrophilic and hydrophobic materials, respectively (Figure S9).

■ CONCLUSION

In this work, three polyesters with the same backbone but side-chains containing various numbers of hydrogen bonding amide-propyl groups (0, 1 and 2) were developed using carbodiimide-mediated coupling of succinic acid and functionalized diols. Effects of amide group derived hydrogen bonding and chain flexibility on thermal, mechanical, and rheological properties were studied. Temperature-dependent FT-IR absorption showed that the hydrogen bond strength decreased with increase of temperature. Hydrogen bonds functioned as supramolecular cross-links, which strengthened the material and limited chain mobility. Having more amide groups in the side-chain raised T_g, stiffness, and brittleness of the material at room temperature. However, influences of hydrogen bonds diminished as temperature increased, and the effect of chain flexibility became more prominent, as shown by rheometry.

DOI: 10.1021/acs.macromol.8b01781
Macromolecules 2018, 51, 9294−9305

This work provides a platform where both effects of hydrogen bonding and chain flexibility can be observed, and the results show that polymer behavior can be modulated by selecting the amount of amide groups in the side-chain and regulating environmental conditions such as temperature and humidity to achieve desirable properties.

■ ASSOCIATED CONTENT

Supporting Information

The Supporting Information is available free of charge on the ACS Publications website at DOI: 10.1021/acs.macromol.8b01781.

Variable temperature-dependent IR spectroscopy, rheological properties, water contact angle measurements, observation of crazing on P(1AP) specimens after tensile testing by optical microscopy and SEM, and structure confirmation of small molecules by ^{1}H NMR and ^{13}C NMR (PDF)

■ AUTHOR INFORMATION

Corresponding Authors

*E-mail: abraham@uakron.edu.
*E-mail: rweiss@uakron.edu.

ORCID

Chao Wang: 0000-0002-5205-9771
Chao Peng: 0000-0002-5672-6324
Amal Narayanan: 0000-0001-8159-6878
R. A. Weiss: 0000-0002-5700-6871
Abraham Joy: 0000-0001-7781-3817

Notes

The authors declare no competing financial interest.

■ ACKNOWLEDGMENTS

The work described herein was funded in part by NSF Grants DMR 1352485 and DMR 1641081.

■ REFERENCES

(1) Hart, L. R.; Li, S.; Sturgess, C.; Wildman, R.; Jones, J. R.; Hayes, W. 3D Printing of Biocompatible Supramolecular Polymers and their Composites. *ACS Appl. Mater. Interfaces* **2016**, *8* (5), 3115−3122.

(2) Wei, P.; Yan, X.; Cook, T. R.; Ji, X.; Stang, P. J.; Huang, F. Supramolecular Copolymer Constructed by Hierarchical Self-Assembly of Orthogonal Host-Guest, H-Bonding, and Coordination Interactions. *ACS Macro Lett.* **2016**, *5* (6), 671−675.

(3) Lu, Y.-S.; Yu, C.-Y.; Lin, Y.-C.; Kuo, S.-W. Hydrogen bonding strength of diblock copolymers affects the self-assembled structures with octa-functionalized phenol POSS nanoparticles. *Soft Matter* **2016**, *12* (8), 2288−2300.

(4) Lübtow, M.; Helmers, I.; Stepanenko, V.; Albuquerque, R. Q.; Marder, T. B.; Fernández, G. Self-Assembly of 9,10-Bis-(phenylethynyl) Anthracene (BPEA) Derivatives: Influence of π-π and Hydrogen-Bonding Interactions on Aggregate Morphology and Self-Assembly Mechanism. *Chem. - Eur. J.* **2017**, *23* (25), 6198−6205.

(5) Chen, Y.; Guan, Z. Multivalent hydrogen bonding block copolymers self-assemble into strong and tough self-healing materials. *Chem. Commun.* **2014**, *50* (74), 10868−10870.

(6) Ahn, B. K.; Lee, D. W.; Israelachvili, J. N.; Waite, J. H. Surface-initiated self-healing of polymers in aqueous media. *Nat. Mater.* **2014**, *13*, 867.

(7) Faghihnejad, A.; Feldman, K. E.; Yu, J.; Tirrell, M. V.; Israelachvili, J. N.; Hawker, C. J.; Kramer, E. J.; Zeng, H. Adhesion and Surface Interactions of a Self-Healing Polymer with Multiple Hydrogen-Bonding Groups. *Adv. Funct. Mater.* **2014**, *24* (16), 2322−2333.

(8) Roy, N.; Tomović, Ž.; Buhler, E.; Lehn, J.-M. An Easily Accessible Self-Healing Transparent Film Based on a 2D Supramolecular Network of Hydrogen-Bonding Interactions between Polymeric Chains. *Chem. - Eur. J.* **2016**, *22* (38), 13513−13520.

(9) Jin, X.; Wang, W.; Xiao, C.; Lin, T.; Bian, L.; Hauser, P. Improvement of coating durability, interfacial adhesion and compressive strength of UHMWPE fiber/epoxy composites through plasma pre-treatment and polypyrrole coating. *Compos. Sci. Technol.* **2016**, *128*, 169−175.

(10) Sijbesma, R. P.; Beijer, F. H.; Brunsveld, L.; Folmer, B. J. B.; Hirschberg, J. H. K. K.; Lange, R. F. M.; Lowe, J. K. L.; Meijer, E. W. Reversible Polymers Formed from Self-Complementary Monomers Using Quadruple Hydrogen Bonding. *Science* **1997**, *278* (5343), 1601−1604.

(11) Brunsveld, L.; Folmer, B. J. B.; Meijer, E. W.; Sijbesma, R. P. Supramolecular Polymers. *Chem. Rev.* **2001**, *101* (12), 4071−4098.

(12) Bentz, K. C.; Walley, S. E.; Savin, D. A. Solvent effects on modulus of poly(propylene oxide)-based organogels as measured by cavitation rheology. *Soft Matter* **2016**, *12* (22), 4991−5001.

(13) Jeffrey, G. A.; Saenger, W. *Hydrogen Bonding in Biological Structures*; Springer: Berlin, 1994.

(14) Aguilar, M. R. *Smart Polymers and Their Applications*; Woodhead: 2017.

(15) McNair, O. D.; Brent, D. P.; Sparks, B. J.; Patton, D. L.; Savin, D. A. Sequential Thiol Click Reactions: Formation of Ternary Thiourethane/Thiol-Ene Networks with Enhanced Thermal and Mechanical Properties. *ACS Appl. Mater. Interfaces* **2014**, *6* (9), 6088−6097.

(16) Gu, J. *Cai liao ke xue yu gong cheng gai lun*; Qing hua da xue chu ban she: Beijing, 2005.

(17) Li, H.; Zhang, C.; Zhang, F. *Gao fen zi wu li*; Zhong guo qing gong ye chu ban she: Beijing, 2009.

(18) Halle, B. Flexibility and packing in proteins. *Proc. Natl. Acad. Sci. U. S. A.* **2002**, *99* (3), 1274−1279.

(19) Teilum, K.; Olsen, J. G.; Kragelund, B. B. Protein stability, flexibility and function. *Biochim. Biophys. Acta, Proteins Proteomics* **2011**, *1814* (8), 969−976.

(20) Jacobs, D. J.; Rader, A. J.; Kuhn, L. A.; Thorpe, M. F. Protein flexibility predictions using graph theory. *Proteins: Struct., Funct., Genet.* **2001**, *44* (2), 150−165.

(21) Ozbas, B.; Rajagopal, K.; Schneider, J. P.; Pochan, D. J. Semiflexible Chain Networks Formed via Self-Assembly of Beta-Hairpin Molecules. *Phys. Rev. Lett.* **2004**, *93* (26), 268106.

(22) Branco, M. C.; Nettesheim, F.; Pochan, D. J.; Schneider, J. P.; Wagner, N. J. Fast Dynamics of Semiflexible Chain Networks of Self-Assembled Peptides. *Biomacromolecules* **2009**, *10* (6), 1374−1380.

(23) Levy, E. D.; Pereira-Leal, J. B.; Chothia, C.; Teichmann, S. A. 3D Complex: A Structural Classification of Protein Complexes. *PLoS Comput. Biol.* **2006**, *2* (11), e155.

(24) Mujika, J. I.; Matxain, J. M.; Eriksson, L. A.; Lopez, X. Resonance Structures of the Amide Bond: The Advantages of Planarity. *Chem. - Eur. J.* **2006**, *12* (27), 7215−7224.

(25) Bhagavan, N. V.; Ha, C.-E. Three-Dimensional Structure of Proteins and Disorders of Protein Misfolding In *Essentials of Medical Biochemistry*, 2nd ed.; Academic Press: San Diego, 2015; Chapter 4, pp 31−51.

(26) Wang, S.-Q. *Nonlinear Polymer Rheology: Macroscopic Phenomenology and Molecular Foundation*; 2018.

(27) Shabbir, A.; Goldansaz, H.; Hassager, O.; van Ruymbeke, E.; Alvarez, N. J. Effect of Hydrogen Bonding on Linear and Nonlinear Rheology of Entangled Polymer Melts. *Macromolecules* **2015**, *48* (16), 5988−5996.

(28) Lewis, C. L.; Stewart, K.; Anthamatten, M. The Influence of Hydrogen Bonding Side-Groups on Viscoelastic Behavior of Linear and Network Polymers. *Macromolecules* **2014**, *47* (2), 729−740.

(29) Osterwinter, C.; Schubert, C.; Tonhauser, C.; Wilms, D.; Frey, H.; Friedrich, C. Rheological Consequences of Hydrogen Bonding:

DOI: 10.1021/acs.macromol.8b01781
Macromolecules 2018, 51, 9294−9305

Linear Viscoelastic Response of Linear Polyglycerol and Its Permethylated Analogues as a General Model for Hydroxyl-Functional Polymers. *Macromolecules* **2015**, *48* (1), 119−130.
(30) Gokhale, S.; Xu, Y.; Joy, A. A Library of Multifunctional Polyesters with "Peptide-Like" Pendant Functional Groups. *Biomacromolecules* **2013**, *14* (8), 2489−2493.
(31) Sperling, L. H.; Sperling, L. H. *Introduction to Physical Polymer Science*; 2015.
(32) Feldman, K. E.; Kade, M. J.; Meijer, E. W.; Hawker, C. J.; Kramer, E. J. Model Transient Networks from Strongly Hydrogen-Bonded Polymers. *Macromolecules* **2009**, *42* (22), 9072−9081.
(33) Messmore, B. W.; Hulvat, J. F.; Sone, E. D.; Stupp, S. I. Synthesis, Self-Assembly, and Characterization of Supramolecular Polymers from Electroactive Dendron Rodcoil Molecules. *J. Am. Chem. Soc.* **2004**, *126* (44), 14452−14458.
(34) Jutier, J.-J.; Lemieux, E.; Prud'homme, R. E. Miscibility of polyester/nitrocellulose blends: A DSC and FTIR study. *J. Polym. Sci., Part B: Polym. Phys.* **1988**, *26* (6), 1313−1329.
(35) Galbiati, E.; Zoppo, M. D.; Tieghi, G.; Zerbi, G. Dipole-dipole interactions in simple esters and in liquid-crystal polyesters. *Polymer* **1993**, *34* (9), 1806−1810.
(36) Carraher, C. E. *Carraher's Polymer Chemistry*; 2018.
(37) Kwei, T. K. The effect of hydrogen bonding on the glass transition temperatures of polymer mixtures. *J. Polym. Sci., Polym. Lett. Ed.* **1984**, *22* (6), 307−313.
(38) Kresheck, G. C.; Scheraga, H. A. The Temperature Dependence of the Enthalpy of Formation of the Amide Hydrogen Bond; the Urea Model1. *J. Phys. Chem.* **1965**, *69* (5), 1704−1706.
(39) Cierpicki, T.; Otlewski, J. Amide proton temperature coefficients as hydrogen bond indicators in proteins. *J. Biomol. NMR* **2001**, *21* (3), 249−261.
(40) Skrovanek, D. J.; Howe, S. E.; Painter, P. C.; Coleman, M. M. Hydrogen bonding in polymers: infrared temperature studies of an amorphous polyamide. *Macromolecules* **1985**, *18* (9), 1676−1683.
(41) Macknight, W. J.; Yang, M. Property-structure relationships in poly-urethanes: Infrared studies. *J. Polym. Sci., Polym. Symp.* **1973**, *42* (2), 817−832.
(42) O'Connell, P. A.; McKenna, G. B. Yield and Crazing in Polymers. In *Encyclopedia of Polymer Science and Technology*; John Wiley & Sons, Inc.: 2002.
(43) Könczöl, L.; Döll, W.; Michler, G. H. Study of the toughening mechanism of crazing in rubber modified thermoplastics. *Colloid Polym. Sci.* **1992**, *270* (10), 972−981.
(44) Dai, X.; Zhang, Y.; Gao, L.; Bai, T.; Wang, W.; Cui, Y.; Liu, W. A Mechanically Strong, Highly Stable, Thermoplastic, and Self-Healable Supramolecular Polymer Hydrogel. *Adv. Mater.* **2015**, *27* (23), 3566−3571.
(45) Wietor, J.-L.; Dimopoulos, A.; Govaert, L. E.; van Benthem, R. A. T. M.; de With, G.; Sijbesma, R. P. Preemptive Healing through Supramolecular Cross-Links. *Macromolecules* **2009**, *42* (17), 6640−6646.
(46) Heinzmann, C.; Salz, U.; Moszner, N.; Fiore, G. L.; Weder, C. Supramolecular Cross-Links in Poly(alkyl methacrylate) Copolymers and Their Impact on the Mechanical and Reversible Adhesive Properties. *ACS Appl. Mater. Interfaces* **2015**, *7* (24), 13395−13404.
(47) Rubinstein, M.; Colby, R. H. *Polymer Physics*; Oxford University Press: Oxford, 2010.
(48) Ferry, J. D. *Viscoelastic Properties of Polymers*; Wiley: New York, 1980.
(49) Thomas, S.; Muller, R.; Abraham, J. *Rheology and Processing of Polymer Nanocomposites*; 2017.
(50) Rogers, S.; Mandelkern, L. Glass Transitions of the Poly-(n-Alkyl Methacrylates). *J. Phys. Chem.* **1957**, *61* (7), 985−991.
(51) Dannis, M. L. Thermal expansion measurements and transition temperatures, first and second order. *J. Appl. Polym. Sci.* **1959**, *1* (1), 121−126.
(52) Barb, W. G. Effect of chemical structure on the softening point of substituted polystyrenes and related materials. *J. Polym. Sci.* **1959**, *37* (132), 515−532.
(53) Shetter, J. A. Effect of stereoregularity on the glass temperatures of a series of polyacrylates and polymethacrylates. *J. Polym. Sci., Part B: Polym. Lett.* **1963**, *1* (5), 209−213.
(54) Tunick, M. H. Activation energy measurements in rheological analysis of cheese. *Int. Dairy J.* **2010**, *20* (10), 680−685.
(55) Collins, E. A.; Metzger, A. P. Polyvinylchloride melt rheology II—the influence of molecular weight on flow activation energy. *Polym. Eng. Sci.* **1970**, *10* (2), 57−65.
(56) Blyler, L. L.; Haas, T. W. The influence of intermolecular hydrogen bonding on the flow behavior of polymer melts. *J. Appl. Polym. Sci.* **1969**, *13* (12), 2721−2733.
(57) Pae, K. *Advances in Polymer Science and Engineering: Proceedings of the Symposium on Polymer Science and Engineering held at Rutgers University, October 26−27, 1972*; Springer: 2012.
(58) Vieira, M. G. A.; da Silva, M. A.; dos Santos, L. O.; Beppu, M. M. Natural-based plasticizers and biopolymer films: A review. *Eur. Polym. J.* **2011**, *47* (3), 254−263.
(59) Ahmed, J.; Rahman, M. S.; Roos, Y. H. *Glass Transition and Phase Transitions in Food and Biological Materials*; Wiley: 2017.

DOI: 10.1021/acs.macromol.8b01781
Macromolecules 2018, 51, 9294−9305